6.0 Performance Improvements Due to Constraints

In this chapter, the performances due to using constraints, those discussed in the last three chapters, are compared for improving MBR distorted images. The cost or the additional information of each constraint is determined to in order to compare improvement per unit cost.

6.1 Additional Information Determination

Some of the constraints discussed in Chapter 3 and 4 need extra information. The amount of the additional information is, in this thesis, computed without taking any statistics into account. The number of bits needed to represent an M-valued discrete of variable additional information is, therefore, $\log_2 M$. Some continuous quantities, such as the energy of the signal for example, need to be quantized before determining the number of bits required for their representation. Note that the MBR constraint and the positivity constraint need no extra information.

6.1.1 Sign/Modified Sign Constraint (C_S)

Since a sign can only be two values, negative or positive, one bit is needed to identify the sign of each pixel value in the error signal. Given j signs for a block of N pixels, the number of additional bits per pixel is j/N. Note that the location information is not necessary since the sign and modified sign projection operator automatically pick the first j locations and the locations which are multiples of N/j respectively. One bit per pixel is required for full description of the signs of the error signals.

6.1.2. Minimum Increasing/Decreasing Constraint (C_{MI}/C_{MD})

For a block of N pixels, the number of bits required to identify each location is $\log_2 N$. The minimum increasing/decreasing values of the error signal, in case of an 8-bit gray scale image, range from 0 to 255. However, the extreme values hardly appear in typical images. Consequently, the upper and lower bound can be reasonably set to 0 to 127 respectively and 7 bits are needed to represent the minimum increasing/decreasing value. Therefore, each block of N pixels requires a total, for J minimum increasing/decreasing locations, of $7+J\cdot\log_2 N$ bits. The number of additional bits per pixel is then $\frac{7 + J \cdot \log_2 N}{N}$. Note that an alternative is to define the minimum increasing/decreasing value globally. Thus, only information on where the minimum increasing/decreasing values are is necessary and 7/N is not required for each block.

6.1.3. Spike Constraint (C_{spk})

Similar to the minimum increasing/decreasing constraints, the spike constraint needs $\log_2 N$ bits for each spike location, 7 bits to identify the spike threshold value and one more bit to specify whether it is a positive or negative spike. The additional number of bits per pixel is then $\frac{8 + J \cdot \log_2 N}{N}$. The amount of additional information needed for this constraint is slightly more than for C_{MI} and C_{MD}.

6.1.4 Slope Constraint (C_{slp})

In the extreme case, the difference between two 8-bit gray scale pixels is 255. Therefore, 8 bits are required for one vector pair. Consider an N×N image which is divided into M×M subimages. The number of internal vertical and horizontal N-pixel-long boundaries is (N/M - 1) for each. If the slope constraint is defined over the full boundaries,

$\frac{8 \times 2 \times \left(\frac{N}{M} - 1 \right)}{N \times N}$ bits per pixel are required as the extra cost for the additional information. On the other hand, if the slope constraint is defined over a part of the full length boundaries, the number of bits per pixel becomes $\frac{8 \times K}{N \times N}$, where K is the total number of the segments that the slope constraint is defined over.

6.1.5 Norm of Slope Constraint (C_{ns})

Although, the norm of the difference vectors is typically high, the value can be normalized by divided by the length of the vector and then quantized to fit into the range 0 to 255. Therefore, 8 bits are needed for each of the vector pair. Thus, this constraint needs the same amount of a priori information as the slope constraint does.

6.2 Effects of Initial Vectors on Performance due to Individual Constraints

Speaking of an individual constraint C, it is implied that the constraint C, the MBR constraint and the positivity constraint cooperate in the reconstruction. The fact is that the information needed for the MBR constraint is already provided by the coefficients. Similarly, positivity of the digital images is known a priori, i.e. without any additional information. As a result, both MBR and positivity constraints are present in all iterative reconstruction. In this implementation, 128×128 images are divided into 16×16 subimages and then compressed by the MBR representation. The MBR distorted images are then iteratively reconstructed by various constraints.

The reconstruction process can be initiated by the observed signal (I_y) itself, the observed signal plus white noise (I_n), the observed signal plus unsent basis vectors (I_u) or even the observed signal plus a constant (I_k). In this section, we are going to find out which initial vector is best suited to each individual constraint.

6.2.1 Constraints Associated with Signs

There are many decoding techniques available to store the information about all the signs. In order to investigate the most appropriate initial vector for this sign constraint C_s, we constrain all pixel signs.

The PSNR's of the reconstructed images using various initial vectors and the sign constraint are shown in Figure 6.1. According to Figure 6.1(a), the PSNR of the final images reconstructed from the observed signal and the sign constraint is not significantly improved. An equal final PSNR is, for this test image, obtained when using the observed signal plus constant (I_k) as the initial vector.

On the other hand, Figure 6.1(a) shows that the white noise added initial vectors (I_n) and the sign constraint, while at first degrading the image PSNR, soon improve PSNR. Some variations are observed from the PSNR due to different realizations of I_n but generally these are significantly higher than the PSNR of I_y.

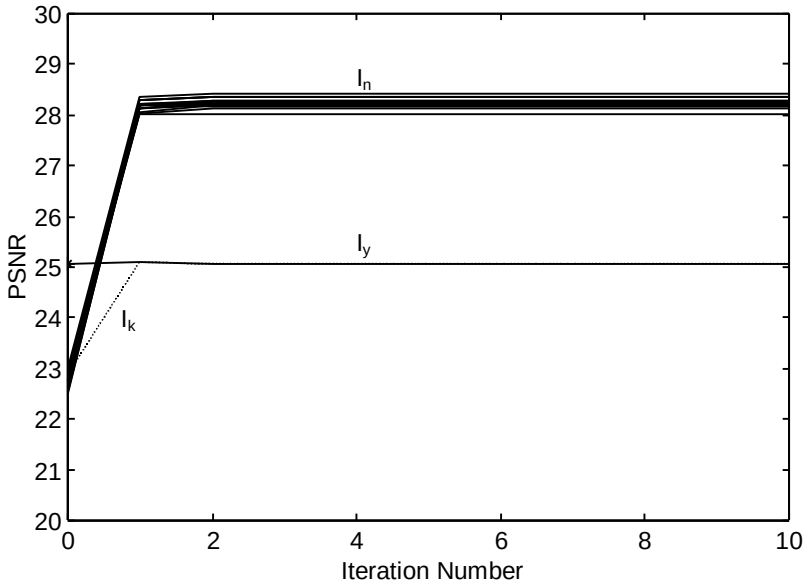

(a) Initiated by observed signal and observed signal plus white noise.

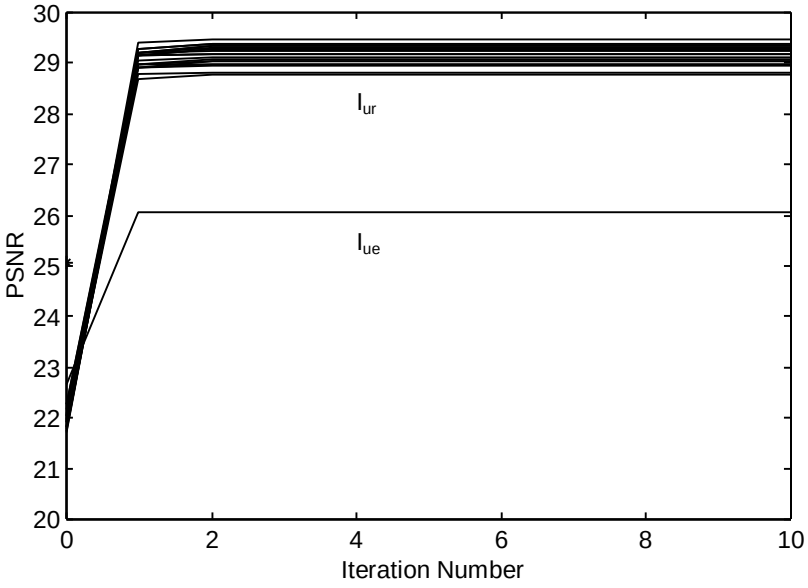

(b) Initiated by observed signal plus unsent basis vectors.

Figure 6.1 PSNR of the images reconstructed by the sign constraint.
(PSNR of observed signal at '*')

Since the observed signal energy is always less than that of the original signal, it makes sense to add some energy to the observed signal. The sign constraint itself does not introduce any energy into the observed signal. Thus, it is not surprising that without adding some energy, the final PSNR obtained from setting the observed signal as the initial vector and invoking only the sign constraint is not comparable to the PSNR from energy-added initial vectors.

Note that some energy is introduced into I_k. However, all added energy is in the DC component only. The DC component is in the subspace of the observed signal, and not in the orthogonal space where the missing energy component are. In other words, the missing energy portion has zero mean. As a matter of fact, the signs are determined after the DC component is removed; furthermore, the DC component is exactly known. Therefore, for this constraint, the results from I_k and I_y are not significantly different or really improved. Nevertheless, the added constant does effect the positivity constraint, which is always included in the reconstruction process.

The best improvement in PSNR is obtained when the observed signal plus the unsent vectors initiate the reconstruction process. Since the gains associated with each unsent vector are not known, they can be either set all to 1 or -1 (I_{ue}) or randomly (I_{ur}). In this implementation, the random coefficients for I_{ur} are uniformly distributed between -1 and 1. The additive vectors are then constrained to a proper energy level that matches the missing energy caused by the MBR compression process. As discussed earlier, we know that the missing energy has zero mean. Because of that all unsent basis vectors are zero mean vectors, so that any linear combinations of them are still zero mean. Thus, both I_{ue} and I_{ur} preserve this zero mean property.

Figure 6.1(b) shows that, with random coefficients, the final results are better than the result from using an equally fixed coefficient gain. Note that the final PSNR of the I_{ur} is a random variable while the PSNR of I_{ue} is a fixed number. Generally, the PSNR's from initiating by I_{ur} are higher than the PSNR from I_{ue}.

Khanna [Khanna 1990] points out that the coefficient distribution can be modeled as a two-sided Gamma function. The equally weighted I_{ue} introduces only the positive side of the distribution. On the other hand, I_{ur} spreads the coefficient to both negative and positive values and the final PSNR's are improved.

Comparing I_n and I_u, at the same added noise variance of 6, the energy added in I_u is guaranteed to be in the subspace, which is orthogonal to the subspace formed by the MBR coefficients. White noise, in general, lies in both subspaces. Some of the energy is shared with the MBR subspace resulting in excess or unwanted noise. Only a portion of the energy is added to the appropriate subspace. We know that the MBR constraint efficiently removes the excess noise in the MBR subspace. The final PSNR of I_{ur} shown in Figure 6.1(b) illustrated higher variation than with I_n, shown in Figure 6.1(a), reflecting the higher noise power in the subspace which is orthogonal to the MBR subspace. Although, the lower bound of the I_{ur} is still higher than the upper bound of the I_n, it is possible to increase the noise power of the I_n to get a final PSNR comparable to those from I_u.

Note that initiating by either I_n or I_u, the PSNR, with the sign constraint, rapidly approaches its final value. Mostly he improvement is achieved by the 3rd iteration. In summary, if only signs are to be constrained, the initial vectors that result in the best PSNR are the observed signal plus either white noise or the unsent basis vector with random

coefficients. The energy level in I_n and I_u plays an important role in reconstruction performances. The influence of the energy level is discussed later.

In addition to the PSNR, the image quality can be determined subjectively. The 64×64 subimage of an original image, illustrated in Figure 6.2(a), show no discontinuity. Some gain, caused by enlarging the image, appears however. The observed image, in Figure 6.2(b), is distorted and severe boundary artifacts are visibly present. The image reconstructed by C_S and I_n, in Figure 6.2(c), contains less blocking artifact but it is still visible. The best subjective quality goes to the image in Figure 6.2(d), which is reconstructed by C_S and I_u. The blocking artifact is reduced. However, blocking artifacts are still visible, especially in the upper right of the image. For this particular image, the PSNR agrees with the subjective evaluation.

Earlier, in order to search for the best initial vector, all signs in the image blocks were constrained. Now the effect of partially constraining the signs and the effect of noise power are to be investigated. Let us choose white noise as the added noise. The average of 10 final PSNR's after 10^{th} iteration versus the number of constrained signs is illustrated in Figure 6.3.

According to Figure 6.3(a), with a small number of signs constrained, the final PSNR is worse than for the observed signal. The final PSNR is roughly 25 dB, according to Figure 6.1(a). The more noise power is added into the observed signal, the more serious the damage to the image. At 128 signs per block, the sign constraint roughly performs, at all noise power levels, the same as when using the observed signal; the improvement is hardly noticeable. Meanwhile, constraining all 256 signs results in a satisfactory PSNR at all noise power levels.

(a) Original Image.

(b) Observed Image.

(c) Reconstructed Image Using C_s and $I_{n.}$

(d) Reconstructed Image Using C_s and I_{ur}.

Figure 6.2 64×64 subimage for subjective evaluation.

As illustrated in Figure 6.3(a), the better final PSNR is achieved when more noise power is added. Therefore, if the iterative reconstruction invokes the sign constraint, it is necessary to have a significant number of signs constrained. Otherwise, the reconstruction process may worsen the final image. Noise power added to the observed signal plays an important role in the iterative reconstruction. If only the signs are constrained, the higher noise power is more effective. However, increasing the energy too much will worsen the PSNR as well. Figure 6.3(b) shows that adding too much energy results in worse final PSNR. The best result was obtained at a noise power level of 6. Beyond $\sigma^2 = 6$, the performance degrades more when a larger amount of noise power is added. Especially, adding high noise power requires more constrained signs to improve the final PSNR.

Theoretically, the added noise power level is suggested to be the same as the residual signal power used as the MBR stopping criterion (16 in this case). However, the implementation shows that the best noise level is different from the one used in the MBR compression. Since the best noise power level can be predetermined at the transmitter end, it is, if the sign constraint is going to be used in the reconstruction process, worth transmitting the best noise level as side information.

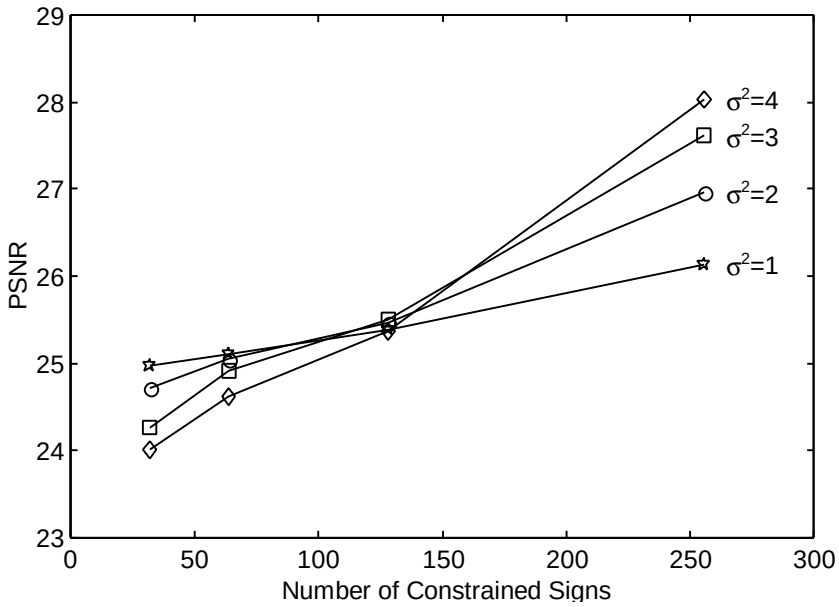

(a) σ^2 from 1 to 4.

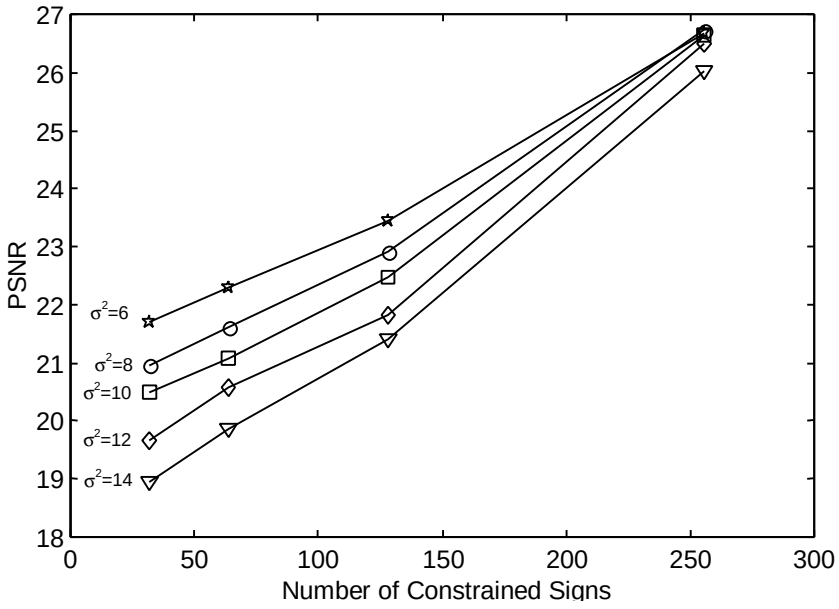

(b) σ^2 from 6 to 14.

Figure 6.3 Performance of the sign constraint at various added noise levels.

6.2.2 Minimum Increasing and Minimum Decreasing Constraint: Energy Added

In this group, the minimum increasing constraint (C_{MI}) and the minimum decreasing constraint (C_{MD}) behave in a similar way; they add energy into the reconstructed image. In order to search for the best initial vector for these functionally-similar constraints, C_{MI32}, the constraint which forces energy to 32 selected minimum increasing locations in the reconstructed signal is chosen as a representative of the constraints in this group.

The performance in terms of PSNR is shown in Figure 6.4. According to Figure 6.4, the best PSNR is achieved when the observed signal I_y itself initiates the iterative image reconstruction process. Initiating with I_k, correspondingly, the PSNR is at first degraded but it quickly approaches the result of I_y. The minimum increasing constraint is defined by the differences of the image pixels. Adding a constant all over the image does not change the differences of adjacent pixel intensities. Once the reconstructed signal was projected onto the MBR subspace, the correct DC component is restored and the reconstructed signal, initiated by I_k, is exactly the same as the one initiated by I_y.

Unlike with the sign constraint, the final PSNR's from added noise initial vectors (both white noise and the biased noise) are not as good as adding no noise. Illustrated in Figure 6.4, a noise variance of 1 is added to the observed signal. Note that this amount of noise is much less than the amount used with the sign constraint in the previous section. The C_{MI32} constraint does not efficiently remove unwanted energy, added by the noise, from the subspace that is orthogonal to the MBR subspace. As a result, the final PSNR is not as good as the result obtained from I_y.

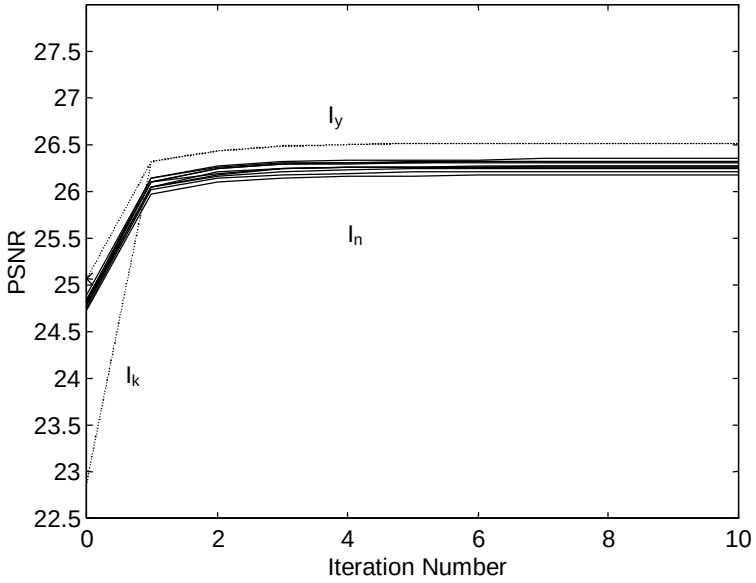

(a) Initiated by observed signal plus noise.

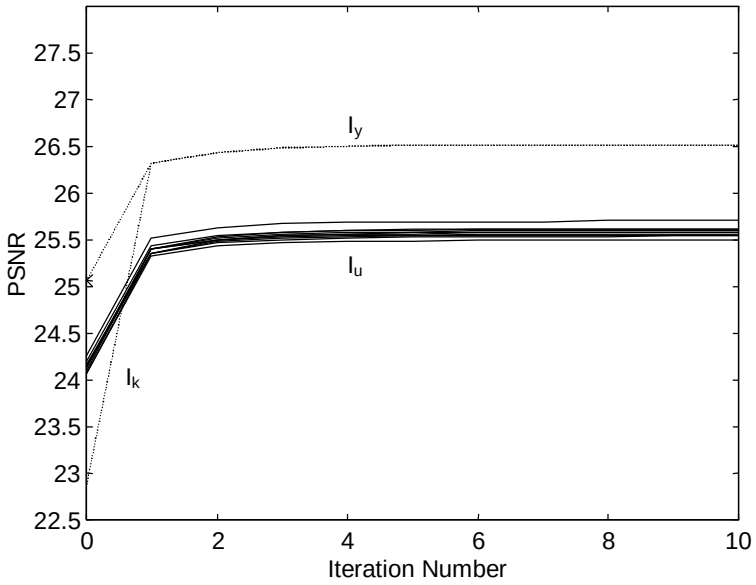

(b) (b) Initiated by observed signal plus unsent basis vectors.

Figure 6.4 PSNR of the images reconstructed by the minimum increasing constraint.

(PSNR of observed signal at "*")

Apparently, the PSNR's with I_u are worse than those with I_n. As a matter of fact, C_{MBR} effectively corrects the signal portion in the MBR subspace but does nothing to the orthogonal subspace. At the same time, the noise-added portion in the orthogonal subspace is insufficiently trimmed toward the original by the C_{MI32} constraint. As a consequence, the results with I_u, which has more energy in the orthogonal subspace, are worse than the results with I_n. Although I_n and I_u yield similar results, one advantage of exploiting I_u is that the amount of energy added into the error signal subspace is known.

The minimum increasing constraint takes roughly 7-8 iterations before the improvement stops. Comparing this constraint and the sign constraint investigated earlier, the rate of convergence of the sign constraint is much faster than the convergence rate of the minimum increasing constraint. Nonetheless, the PSNR hardly improves after the 4^{th} iteration.

6.2.3 Spike Constraint: Compromising

In the last two subsections we found that of the noise added vectors either I_n or I_u is the best initial vector for the sign constraint, while the observed signal I_y is the most appropriate for the minimum increasing and minimum decreasing constraints. Let use next consider the spike constraint. This constraint does add energy to the reconstructed vectors and at the same time it automatically constrains the signs of the spike and the two adjacent pixels. Consequently, it is not obviously justifiable which initial vector would serve this constraint best.

By observation of typical subimages, spikes with high intensity are not found often. In this implementation on blocks of size 16×16, a maximum of 32 spikes are to be

constrained for each block (C_{spk32}). However, the total number of spikes in a block is possibly less than 32. In this case, all spikes found in the block will be constrained.

The final PSNR's resulting from use of the spike constraint, are shown in Figure 6.5. The results with this constraint are similar to the results with the minimum increasing constraints rather than those with the sign constraint. Comparing the final PSNR's of using I_y and I_n with C_{spk32}, in Figure 6.5(a), the former initial vector I_y yields more improvement than the latter.

Unlike the sign and minimum increasing constraints, the PSNR from using the spike constraint is influenced by increasing or decreasing the DC component. The best performance of the spike constraint, on this particular image, is obtained when I_k is invoked for the initial vector. Figure 6.5(b) illustrates the results from using I_k. In this implementation, adding both constant 1 and -1 into the observed signal results in more improvement than using the observed signal itself. Nevertheless, overusing the added constant, say 2 or -2 in Figure 6.5(b), results in a worse PSNR as well. It is not obvious whether a positive or negative constant produces better performance. Therefore, it is worth it to include the constant that is the best for each particular image. Note that the possible constant that can be added to the discrete observed signal must practically be an integer. Thus, DC noise power is then discrete too; it must be the square of integers, for instance, 1, 4, 9 etc. This limits the freedom in assigning a noise level.

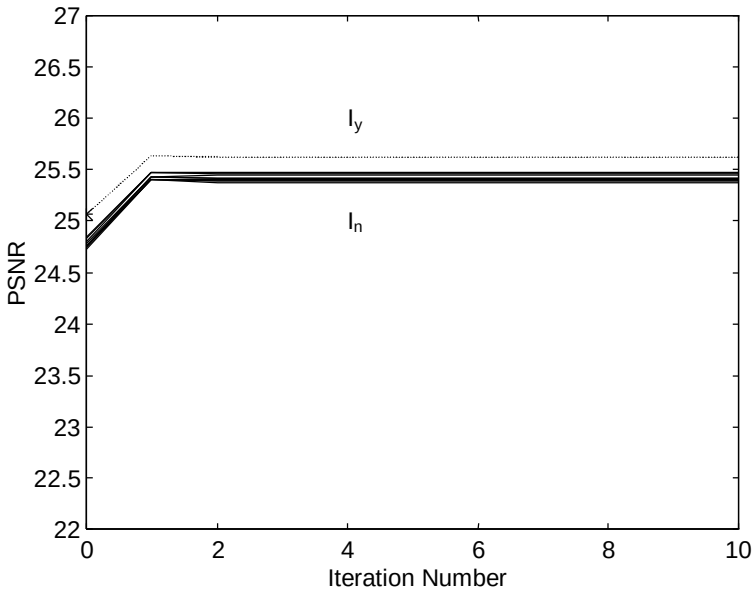

(a) Initiated by I_y and I_n.

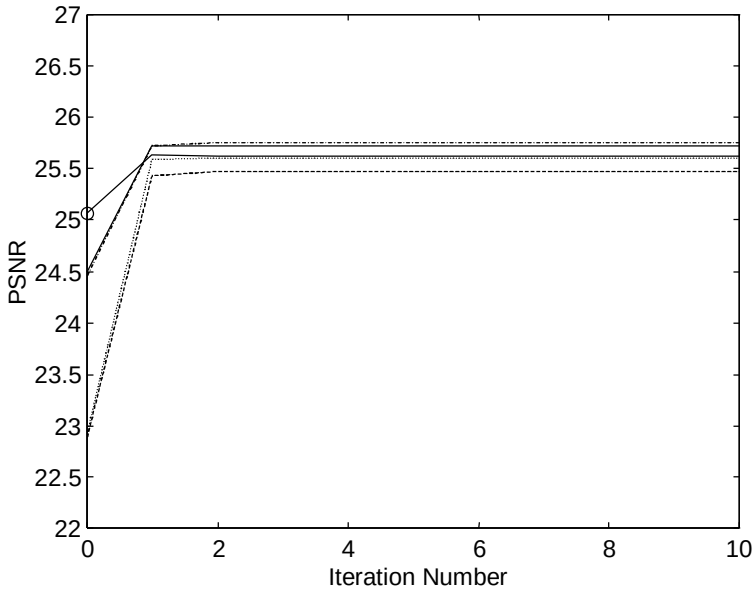

(b) Initiated by I_k.

[k=1: solid, k=-1: dash and dot, k=2: dot, k=-2: dash, k=0(Iy): circle)]

Figure 6.5 PSNR of the images reconstructed by the spike constraint.

As discussed in Section 6.2.1, the number of constrained signs that causes improved PSNR must be large enough. According to the 32-location spike constraint (C_{spk32}), the number of signs to be constrained is at most 96 which is far less than sufficient (see Figure 6.3) for a block of size 256. Thus, the constrained signs in C_{spk32}, are not very effective. Given the same number of energy-added locations, C_{MI32} outperforms C_{spk32} in the reconstruction initiated by I_y. It reflects that C_{MI32} more efficiently inserts missing energy into the reconstructed signal than C_{spk32} does. The minimum increasing constraint is defined over the locations where the largest differences of pixel intensity are found. The spike is restricted by the sign change and thus the locations of spikes do not guarantee largest energy. Moreover, C_{spk} adds energy to one pixel while C_{MI} and C_{MD} add energy to two adjacent pixels simultaneously.

Figure 6.6 compares the original and reconstructed images from different constraints initiated with the most appropriate initial vectors. The sign constraint and the initial vector I_n, shown in Figure 6.6(b), produces the best result both objectively (29.04 dB PSNR) and subjectively (less visible distortion on the block boundaries). The resulting images due to the C_{MI32} constraint with I_y (26.53 dB PSNR) and the C_{spk32} constraint with I_k (27.76 dB PSNR) are shown in Figure 6.6(c) and (d) respectively. Note that the poor discontinuities at the boundaries are not efficiently removed.

(a) Original image.

(b) I_{ur} and C_{sgn}, 29.04 dB PSNR.

(c) I_y and C_{MI32}, 26.52 dB PSNR.

(d) I_k and C_{spk32}, 25.76 dB PSNR.

Figure 6.6 Comparison of the reconstructed images.

6.3 Performance Improvements Due to the Boundary Constraints

The constraints evaluated in this section are implemented over pixels that form block boundaries. All other pixels are only constrained by the MBR and sign constraints. In addition to the overall PSNR, the PSNR computed over the boundary pixels, resulting from each boundary constraint, are compared.

6.3.1 Slope Constraint: Correct Discontinuity

The three groups of constraints discussed in Section 6.2, with a proper initial vector, improve the overall reconstructed images both in PSNR and subjective measurement. Nonetheless, the poor edge discontinuity is still visible. Let us start with a simple constraint C_{slp0}. The slope constraint, C_{slp0}, solves the blocking artifact problem by averaging the pixels hat form the boundaries. Since a zero difference between the boundary pixels is assumed, no additional information is required for this constraint. The effectiveness of this constraint, in terms of the overall and the boundary PSNR, is illustrated in Figure 6.7(a) and (b) respectively. Note that the PSNR associated with the noise added initial vector, I_n, is computed by taking the average of 20 realizations.

We assume, with C_{slp0}, that the difference between the pixels that form the block boundaries are zero. In reality, this assumption is generally wrong. Figure 6.7 shows that C_{Slp0} does improve the image PSNR, especially the overall PSNR, even though the assumption of a zero pixel difference is wrong for the test image. The best results re achieved by using the observed signal as the initial vector.

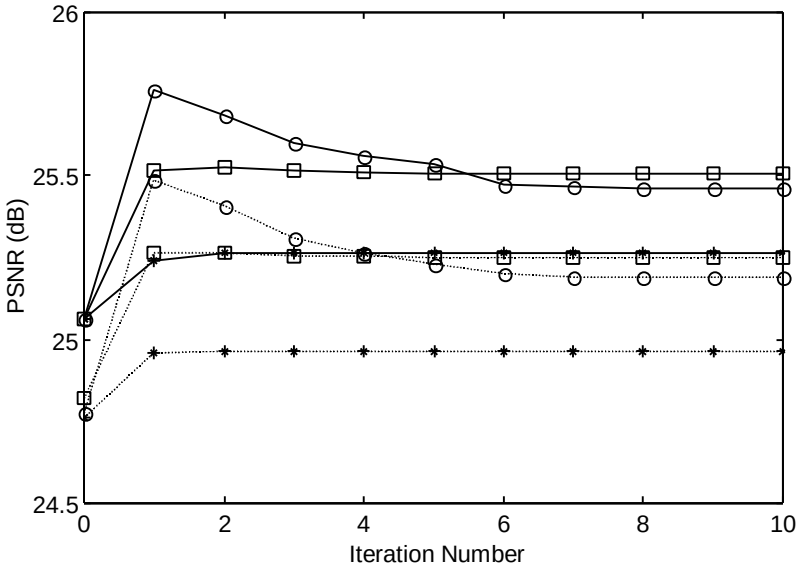

(a) Overall PSNR.

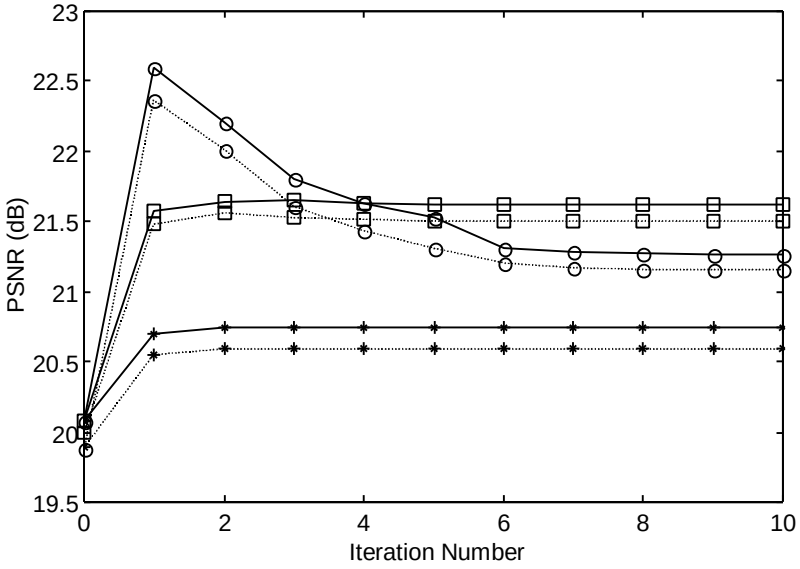

(b) Boundary PSNR.

Legend:
—o— I_y and C_{slp0}
—*— I_y and C_{slp64}
—[]— I_y and C_{slp16}
···o··· I_n and C_{slp0} (average)
···*··· I_n and C_{slp64} (average)
···[]··· I_n and C_{slp16} (average)

Figure 6.7 PSNR of the images reconstructed by the slope constraint.

Without the assumption of zero pixel difference, the actual maximum absolute slope is included in the C_{slp} constraint. Note that the signs of the slop are not included in this constraint. Since we have freedom to choose that length of the boundary vector to be constrained, in this implementation, C_{slp16} and C_{slp64} (which implement the slope constraint over a boundary length of 16 and 64 respectively) are used to compare the results. According to Figure 6.7, constraining over a long boundary C_{slp64}, is less efficient than constraining over a shorter length C_{slp16}. However, C_{slp16} does need more side information than C_{slp64}. In summery, the shorter the constrained boundary length, the better the performance.

As shown in Figure 6.7(a), the final overall PSNR resulting from C_{slp0} is nearly as good as that from of C_{slp16}. However, if the improvement at the boundary is compared, as in Figure 6.7(b), C_{slp16} outperform C_{slp0} no mater which initial vectors are used. Note from Figure 6.7(b) that the boundary pixel PSNR does not suffer much from adding noise to the observed signal. The final boundary PSNR's resulting from the observed signal exceed those resulting from noise added initial vectors by only a little bit. As a consequence, this constraint should cooperate well with the constraint that need noise to be added into the observed signal, e.g., the sign constraint.

6.3.2 Norm-of-Slope Constraint

Comparing the overall PSNR of the observed signal to the boundary PSNR of the same signal, the boundary PSNR is significantly lower than the overall PSNR. This implies that efficiently increasing PSNR at the boundary yields an improvement of the overall PSNR. In the previous section, the overall PSNR of images reconstructed by using the

maximum slope constraint improved the overall PSNR by roughly 0.5 dB and the boundary PSNR by 1.5 dB. The slope constraint does improve the PSNR at the boundary but the performance is still fare from satisfactory.

As discussed in Chapter 4, the length of the boundaries to be constrained can be defined differently. To compare the performance of the slope constraint to the norm-of-slope constraint fairly, the lengths of the constrained boundary vectors are assigned exactly as in Section 6.3.1. Let us denote C_{NS16} as the norm-of-slope constraint implemented on vectors of length 16 and 64 respectively. The reconstruction process is initiated either by the observed signal I_y or the observed signal plus noise I_n.

Figure 6.8 illustrates the PSNR resulting from all four combinations of the initial vectors I_n, I_y and the constraints C_{NS16}, C_{NS64}. Note that the PSNR associated with I_n is the average value of 20 PSNR realizations. Both the overall PSNR and the boundary PSNR achieve their maximum when the length of the constrained boundary vectors is short. The longer the length, the worse PSNR. Moreover, as in the case of the slope constraint, adding noise worsens the overall PSNR. In this implementation, a white noise variance of 1 is added, causing the overall PSNR (in both the length of 16 and 64 cases), to deteriorate by 0.5 dB relative to using the observed signal only.

Now, let us consider the boundary PSNR. As illustrated in Figure 6.8(b), the effect of added noise does not play a major role in the performance degradation in this region. The performance mainly depends on the length of the constrained boundary vectors. The shorter length provides a more accurate norm value and the constraint is then more effective. This is a nice property of this constraint because it can cooperate well with the sign constraint, which needs additive noise in the image reconstruction.

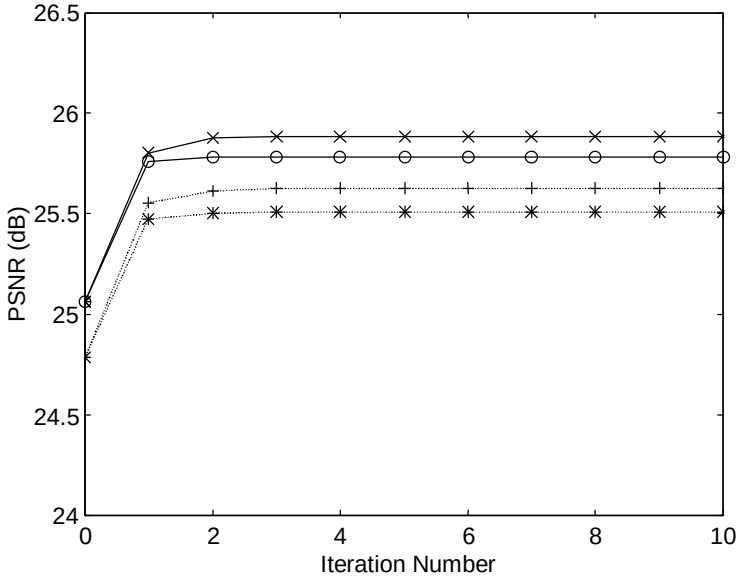

(a) Overall PSNR.

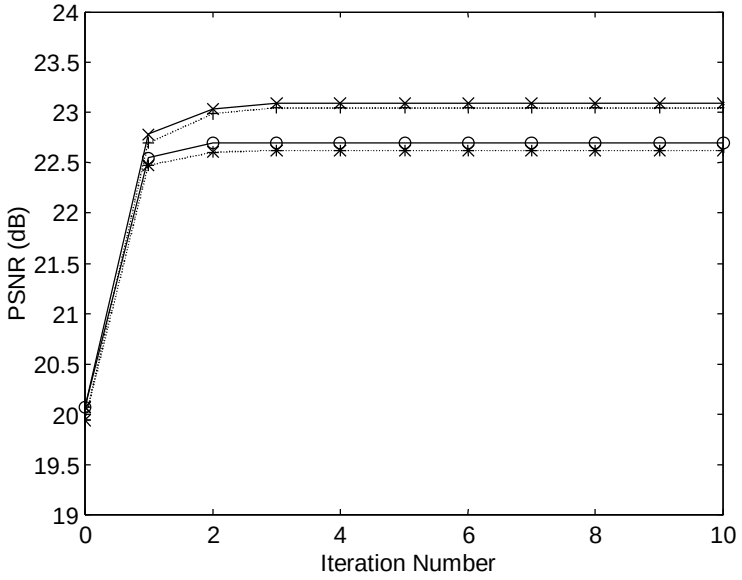

(b) Boundary PSNR.

Legend: —x— I_y and C_{NS16} …+… I_n and C_{NS16} (average)
—o— I_y and C_{NS64} …*… I_n and C_{NS64} (average)

Figure 6.8 Performance due to the norm-of-slope constraint with actual norms.

Although, the overall PSNR is improved by only 1 dB, the PSNR at the boundary is improved by an impressive 3 dB. Subjectively, the norm-of-slope constraint efficiently removes the blocking artifacts, especially when two adjacent blocks are in the same texture region. However, if two adjacent blocks are in different brightness (edge) regions, i.e. with significantly different DC levels, the blocking artifacts are still noticeable. As illustrated in Figure 6.11(b), the discontinuities under the eye are almost invisible but on the upper right of the eye there are strong artifacts.

6.3.3 Norm-of-Slope Constraint with Estimated Norm

We know, from the previous two sections, that constraining shorter length boundary vectors results in a better PSNR. However, the shorter length means that more information must be included with the transmitted signal. It would be nice if the estimated norm value could be determined efficiently from the observed signal itself.

Figure 6.9 illustrates the value of the actual length-of-16 boundary norms from the original image and the estimated norms computed from the observed signal as discussed in Chapter 4. For this image, the actual norms are most likely to have a higher value than the estimated norms. To compare the performance, the same image as in Section 6.3.2 is constrained by the estimated norms and the results in terms of PSNR are illustrated in Figure 6.10. Comparing with the results depicted in Figure 6.8, using the estimated norms, for this test image, surprisingly results in better PSNR especially when the observed signal is the initial vector and the shorter length boundary vector constraint is used. However, the results from using the actual norms and utilizing the estimated norms are not significantly different if the initial vector is I_n.

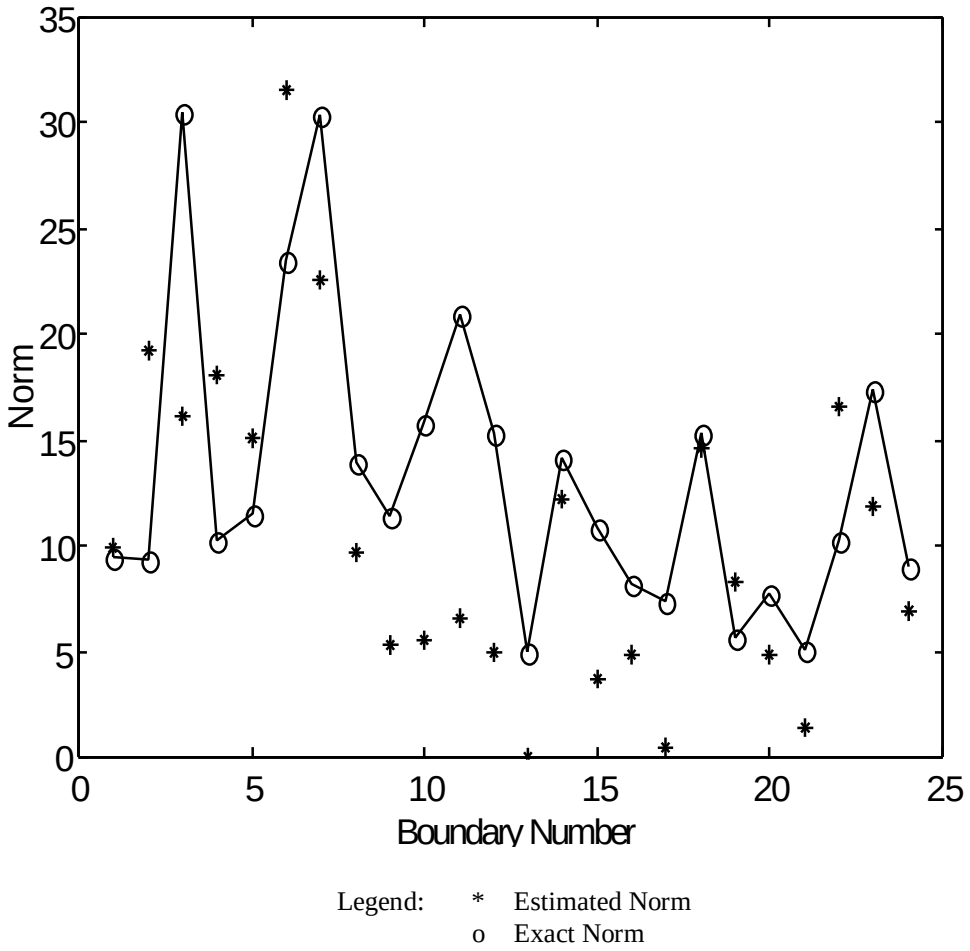

Figure 6.9 Exact and estimated boundary norm values.

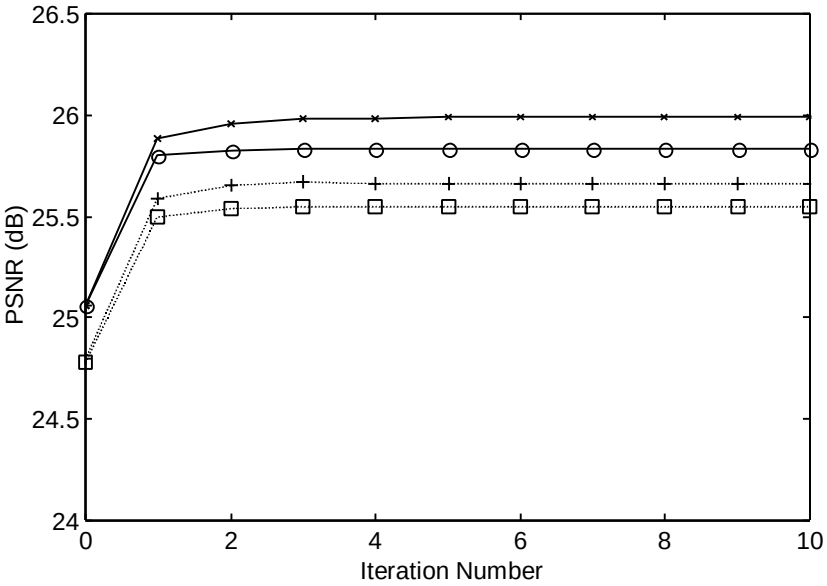

(a) Overall PSNR.

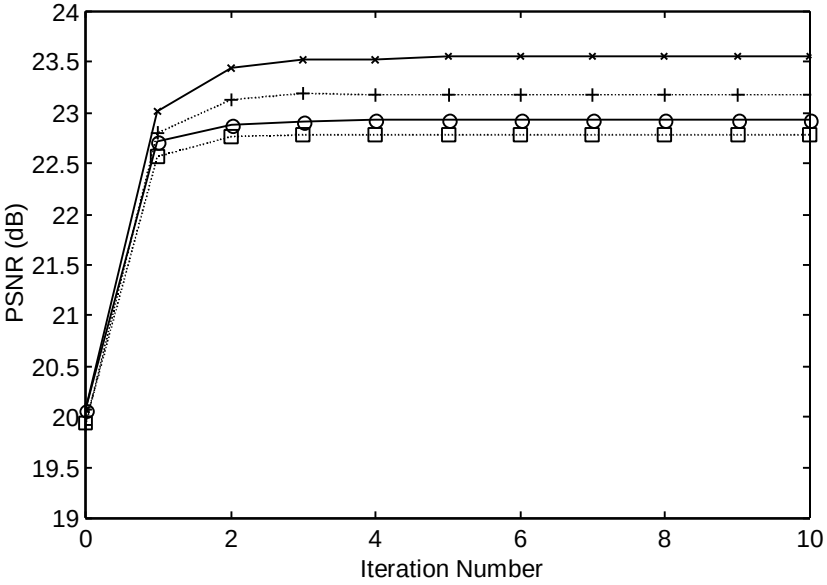

(b) Boundary PSNR.

Legend: —x— I_y and C_{NS16} ···+··· I_n and C_{NS16} (average)
—o— I_y and C_{NS64} ···ð··· I_n and C_{NS64} (average)

Figure 6.10 Performance due to the norm-of-slope constraint with estimated norms.

(a) Original image.

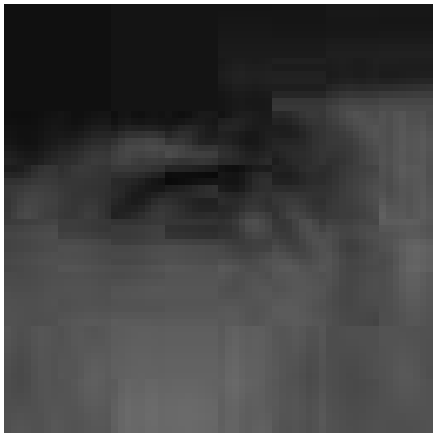

(b) C_{slp16}, I_y (21.62 dB PSNR).

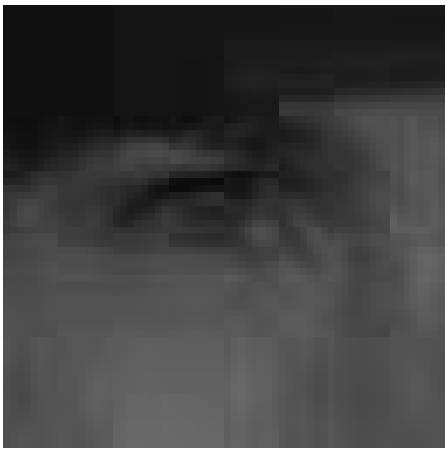

(c) C_{NS16} with Exact Norms, Iy (23.09 dB PSNR).

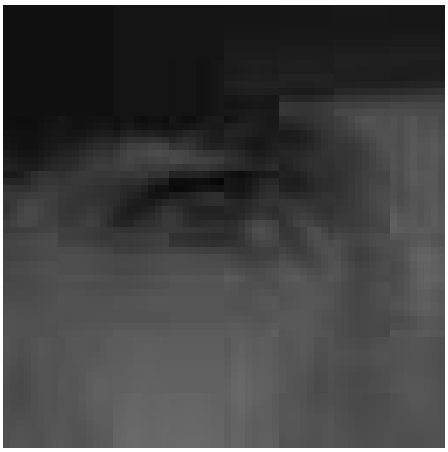

(d) C_{NS16} with Estimated Norms, Iy (23.56 dB PSNR).

Figure 6.11 Comparison of the images reconstructed by the boundary constraints.

Figure 6.11 compares the reconstructed images resulting from the constraints associated with the boundaries. Comparing Figure 6.11(c) and (d), the latter shows less discontinuity at the block boundaries than the former. This subjective result agrees with the boundary PSNR illustrated in Figure 6.10(b). According to Figure 6.9, the estimated norms of slope are most likely less than the actual value. Thus, using the estimated norms, the boundaries are enforced more strongly than when the actual norm values are used. Note that, in this implementation, quantization, which we do not intensively discuss, does influence the results. Thus, it is possible that using the estimated norms produces better performance than using the actual norms.

In summary, the estimated norms computed from the observed signal are good enough for the norm-of-slope constraint. Apparently, the use of none of the estimated norms worsens the final PSNR compared to the results from using the actual norms.

6.4 Implementation on Other Images

Previously, in Sections 6.2 and 6.3, the most appropriate initial vector for each constraint is determined. In this section, the constraints and their most appropriate initial vectors are used to reconstruct a landscape and an X-ray image, from the distorted MBR representation.

Tables 6.1 and 6.2 summarize the improvement of the overall and boundary final PSNR's respectively, of the test images. For these particular images, the minimum increasing/decreasing constraints outperform the spike constraint both in overall and boundary PSNR. In the meanwhile, the norm-of-slope constraint, on all images, provides better results than the slope constraint does. Unlike the results for the portrait image, using

the actual norm values with the norm-of-slope constraint, on the landscape and X-ray images, improves the final PSNR's more than using the estimated values. Thus, using the estimated norm value does not work well for every image.

Typically, by observation, a severe blocking artifact occurs when the DC components of two adjacent blocks are significantly different. In general, X-ray images consist of some extremely bright regions neighbored by extremely dark regions. Thus, the boundary PSNR on MBR distorted X-ray images is, with the MSE stopping criterion, typically low compared to other images (see Table 6.2). The minimum increasing/decreasing locations on the error signal of X-ray images would be along the boundary of the extremely dark and bright regions. Adding energy to the border highlights the differences of the dark and bright regions. Therefore, the minimum increasing/decreasing constraints are good choices for X-ray images.

In general, the improvements in terms of boundary PSNR are significantly higher than in terms of the overall PSNR. However, the results from the sign constraint are different. By using the sign constraint, both overall and boundary PSNR's (Tables 6.1 and 6.2) are, roughly speaking, equally improved (in dB). In other words, the sign constraint uniformly improves the entire image, not in particular only at the boundary. In addition, the boundary PSNR improvement due to the sign constraint, is almost as good, on all test images, as either one of the norm-of-slope constraints, which is aimed specifically at removing the boundary discontinuity. Figure 6.12 and 6.13 compare the final images.

Table 6.1 Improvement of overall PSNR (dB) from the MBR observed signal.

Constraint and Initial Vector	Portrait (25.06 dB Observed)	Landscape (26.66 dB Observed)	X-ray (26.29 dB Observed)
C_{S256} and I_n (average)	3.12	2.94	2.79
C_{MI32} and I_y	1.46	1.03	1.72
C_{MD32} and I_y	1.47	1.27	1.67
Cs_{pk32} and I_k	0.50	0.42	0.86
C_{slp16} and I_y	0.45	0.50	0.94
C_{NS16} and I_y (actual norm)	0.83	0.70	1.16
C_{NS16} and I_y (estimated norm)	0.93	0.66	1.02

Table 6.2 Improvement of boundary PSNR (dB) from the MBR observed signal.

Constraint and Initial Vector	Portrait (20.07 dB Observed)	Landscape (22.82 dB Observed)	X-ray (19.32 dB Observed)
C_{S256} and I_n (average)	3.03	3.16	2.77
C_{MI32} and I_y	2.29	1.90	3.12
C_{MD32} and I_y	2.24	2.32	2.77
Cs_{pk32} and I_k	1.22	0.69	1.63
C_{slp16} and I_y	1.55	2.90	2.70
C_{NS16} and I_y (actual norm)	3.02	3.19	3.46
C_{NS16} and I_y (estimated norm)	3.49	3.05	2.79

(a) Original landscape image.

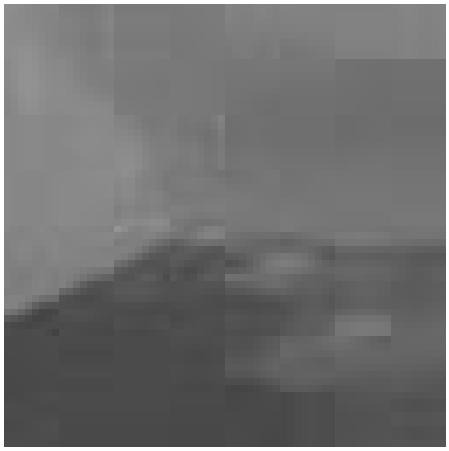

(b) C_{S256} (29.60 dB ovl & 25.97 dB bnd).

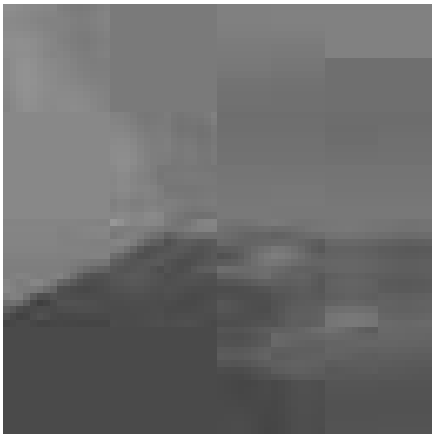

(c) C_{MD32} (27.97 dB ovl & 25.14 dB bnd).

(d) C_{NS16} (27.37 dB ovl & 26.01 dB bnd).

[ovl = overall, bnd = boundary]

Figure 6.12 Reconstructed landscape images.

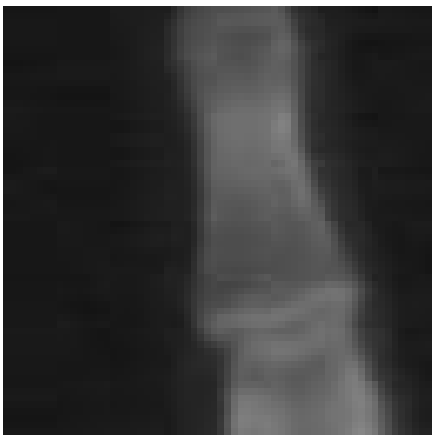

(a) Original X-ray image.

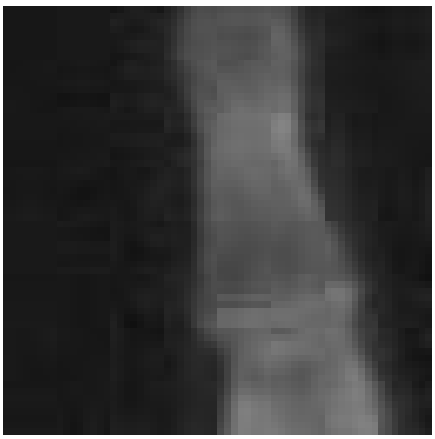

(b) C_{S256} (29.05 dB ovl & 22.09 dB bnd).

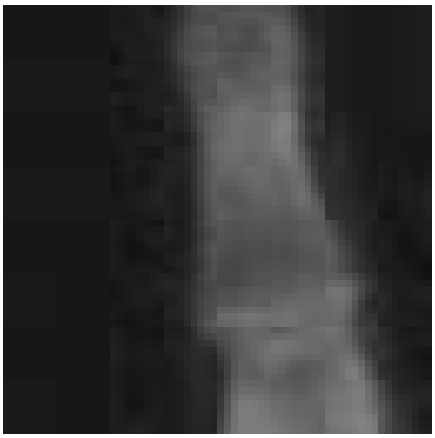

(c) C_{MI32} (28.01 dB ovl & 22.44 dB bnd).

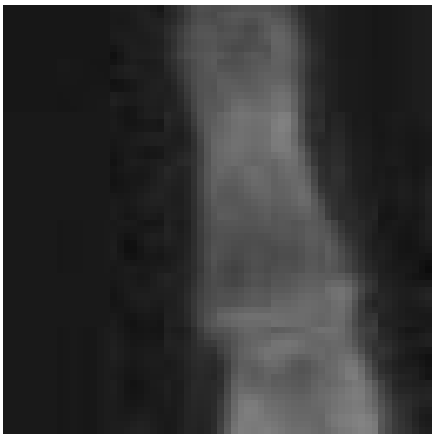

(d) CNS16 (27.45 dB ovl & 22.78 dB bnd).

[ovl = overall, bnd = boundary]

Figure 6.13 Reconstructed X-ray images.

6.5 Sequence of Projection Operators

Previously, in Sections 6.2 and 6.3, only one constraint was used to reconstruct the MBR distorted images. In this section, multiple constraints are used and the performances of different projection sequences are compared.

The sign constraint, the maximum increasing constraint and the norm-of-slope constraint are invoked for this sequence test. The strategy of implementing the composite projection is that two constraints (selected from the three mentioned) and the MBR constraint make up the composite constraints. In this implementation, the MBR constraint is designated to be the last constraint of the composite projections. Thus, the total number of the combinations is six. Note that the positivity constraint is automatically implemented by the pixel representation format (0 to 255).

Since the sign constraint does not perform well without added noise, and the rest of the constraints does not suffer much from that noise, any composite projections with the sign constraint are initiated by the observed signal plus noise, I_n. In this investigation, for the composite projections associated with the sign constraint, the average of 20 realizations is used in the comparison. The composite projection of the minimum increasing/decreasing and the norm-of-slope constraints, in this implementation, invokes the observed signal as the initial vector.

Tables 6.3 and 6.4 show, respectively, the overall and boundary PSNR of the reconstructed images from the different sequences of the composite projection operators after the 10^{th} iteration. Figure 6.14 illustrates the improvement of PSNR of the landscape image as a result of using different composite projection operators.

Table 6.3 Overall PSNR of different projection sequences

Projection Operator, Initial vector	Portrait (25.06 dB Observed)	Landscape (26.66 dB Observed)	X-ray (26.29 dB Observed)
$P_{MBR}P_{MI}P_{MD}P_S$, I_n	5.83	5.33	5.70
$P_{MBR}P_SP_{MI}P_{MD}$, I_n	5.71	5.23	5.70
$P_{MBR}P_{NS}P_S$, I_n	4.18	3.84	4.51
$P_{MBR}P_SP_{NS}$, I_n	4.20	3.86	4.52
$P_{MBR}P_{NS}P_{MD}P_M$, I_y	3.14	2.54	3.22
$P_{MBR}P_{MI}P_{MD}P_{NS}$, I_y	3.15	2.47	3.41

Table 6.4 Boundary PSNR of different projection sequences

Projection Operator, Initial vector	Portrait (20.07 dB Observed)	Landscape (22.82 dB Observed)	X-ray (19.32 dB Observed)
$P_{MBR}P_{MI}P_{MD}P_S$, I_n	6.66	6.55	7.32
$P_{MBR}P_SP_{MI}P_{MD}$, I_n	6.49	6.52	7.21
$P_{MBR}P_{NS}P_S$, I_n	6.81	7.50	8.33
$P_{MBR}P_SP_{NS}$, I_n	6.70	7.35	8.27
$P_{MBR}P_{NS}P_{MD}P_M$, I_y	6.30	6.15	8.08
$P_{MBR}P_{MI}P_{MD}P_{NS}$, I_y	6.19	5.60	7.05

According to Tables 6.3 and 6.4, ordering of the projection does not affect the final PSNR's very much. However, the results illustrate that constraining the signs followed by using the minimum increasing/decreasing constraint yields slightly better results, on all test images, than using reverse order.

Let us consider the performance of the norm-of-slope constraint on the boundary PSNR. The results suggest that in order to improve the boundary PSNR, the norm-of-slope constraint should be applied after the minimum increasing/decreasing or sign constraints. The results, however, do not always imply better overall PSNR's.

In summary, the results suggest that the sign constraint should be implemented first, then the minimum increasing/decreasing constraint, and finally the norm-of-slope constraint.

Figure 6.14 shows the characteristics of the PSNR improvement on the landscape image. In the first iteration, the projection sequence plays an important role in PSNR improvement. However, the final results of the different projection sequences after a couple of iterations are not significantly different.

According to Table 6.3, $P_{MBR}P_{MI}P_{MD}P_{S}$ outperforms, in terms of the overall PSNR improvement, $P_{MBR}P_{NS}P_{S}$ and $P_{MBR}P_{MI}P_{MD}P_{NS}$. Roughly speaking, the PSNR improvement differences between each composite projection is about 1-1.5 dB, thus leaving around 2-3 dB between the PSNR of using $P_{MBR}P_{MI}P_{MD}P_{S}$ and $P_{MBR}P_{MI}P_{MD}P_{NS}$, the best and worst composite projections respectively. However, the boundary PSNR's resulting from using those composite constraints on the test images are insignificantly different.

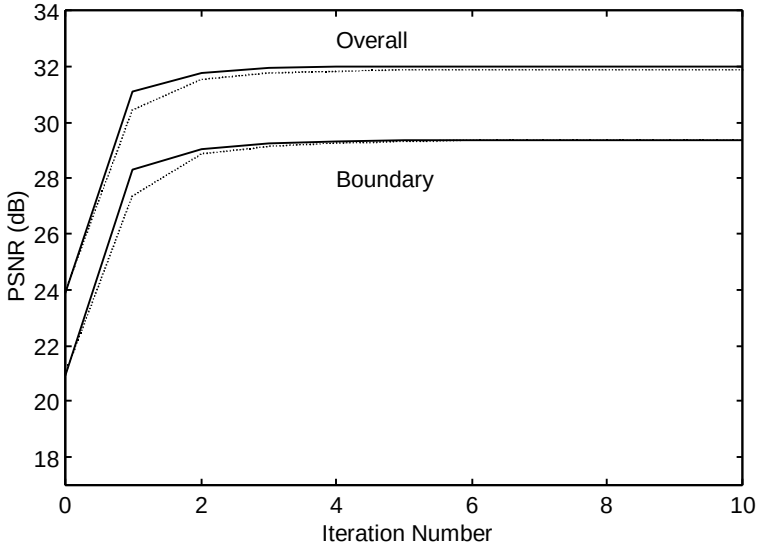

(a) dot: $P_S P_{MD} P_{MI}$ solid: $P_{MI} P_{MD} P_S$

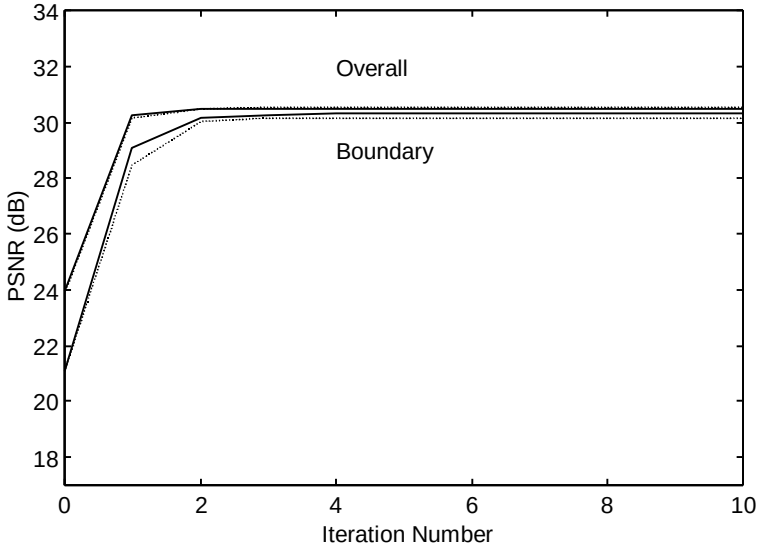

(b) dot: $P_S P_{NS}$, solid: $P_{NS} P_S$

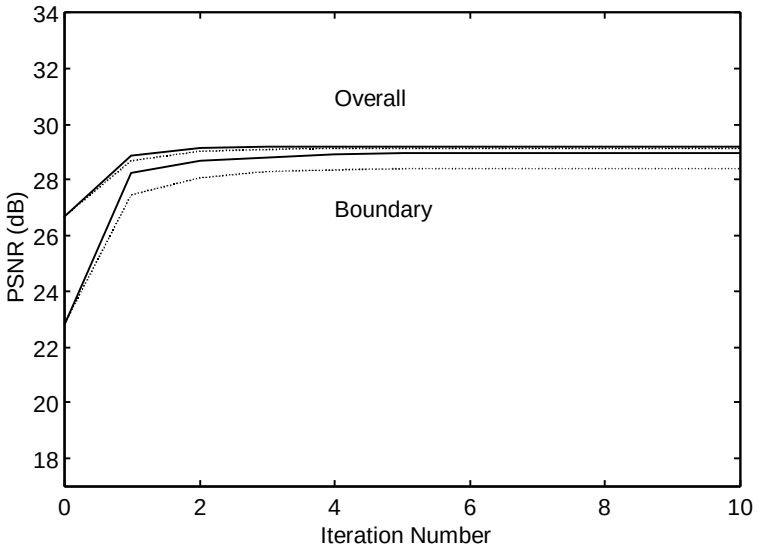

(c) dot: $P_{MI}P_{MD}P_{NS}$, solid: $P_{NS}P_{MD}P_{MI}$

Figure 6.14 PSNR of different projection sequences used on the landscape image.

Figures 6.15-17 show the reconstructed images using the composite constraints discussed in this section. Although $P_{MBR}P_{MI}P_{MD}P_S$ denotes the best overall PSNR for all test images, without a very close look, it is hard to tell subjectively which reconstructed image is the best. Moreover, the reconstructed images with higher boundary PSNR subjectively provide a little bit better final image. For this reason, it is recommended to invoke the norm-of-slope constraint.

(a) Original.

(b) $P_{MBR}P_{MI}P_{MD}P_S$

(30.89 dB ovl, 26.73 dB bnd).

(c) $P_{MBR}P_{NS}P_S$

(29.24 dB ovl, 26.88 dB bnd).

(d) $P_{MBR}P_{NS}P_{MD}P_{MI}$

(28.20 dB ovl, 26.37 dB bnd).

[ovl = Overall, bnd = Boundary]

Figure 6.15 Reconstructed portrait images by using composite constraints.

(a) Original landscape image.

(b) $P_{MBR}P_{MI}P_{MD}P_S$

(31.99 dB ovl, 29.37 dB bnd).

(c) $P_{MBR}P_{NS}P_S$

(30.50 dB ovl, 30.32 dB bnd).

(d) $P_{MBR}P_{NS}P_{MD}P_{MI}$

(29.20 dB ovl, 28. 97 dB bnd).

[ovl = Overall, bnd = Boundary]

Figure 6.16 Reconstructed landscape images by using composite constraints

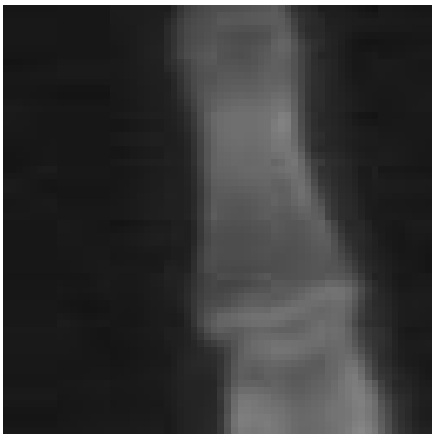

(a) Original X-ray image.

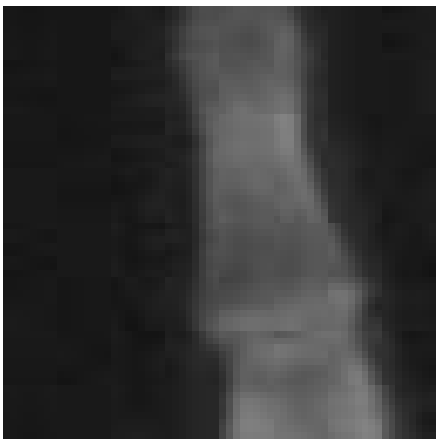

(b) $P_{MBR}P_{MI}P_{MD}P_S$

(31.99 dB ovl, 26.64 dB bnd).

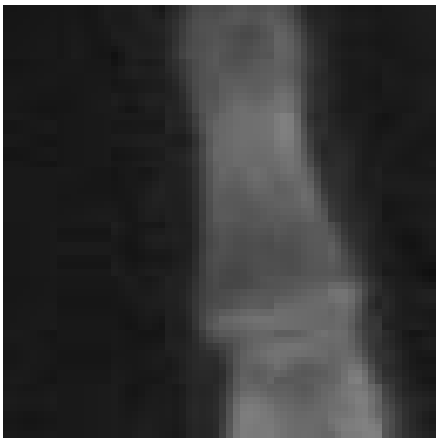

(c) $P_{MBR}P_{NS}P_S$

(30.80 dB ovl, 27.65 dB bnd).

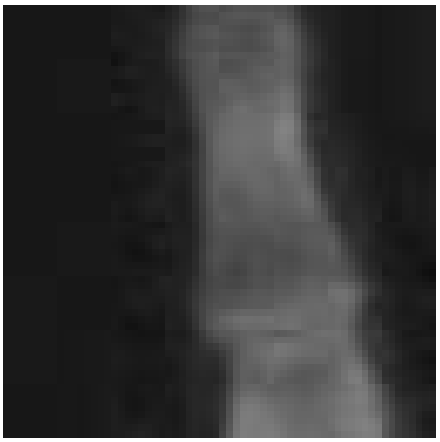

(d) $P_{MBR}P_{NS}P_{MD}P_{MI}$

(29.51 dB ovl, 27.40 dB bnd).

[ovl = Overall, bnd = Boundary]

Figure 6.17 Reconstructed X-ray images by using composite constraints.